International Journal of Engineering Inventions
e-ISSN: 2278-7461, p-ISSN: 2319-6491
Volume 15, Issue 11 [November 2026] PP: 41-48

Study of Crystal Field Energy Levels and Zero Field Splitting Parameters of Mn^{2+}: $NiK_2 (SO_4)_2 \bullet 6H_2O$ Single Crystals

Ram Kripal
EPR Laboratory, Department of Physics, University of Allahabad, Prayagraj-211002, India

Abstract
Using the superposition model (SPM), the crystal field (CF) and zero field splitting (ZFS) properties of Mn^{2+} doped Ni $K_2 (SO_4)_2.6H_2O$ (NKS) single crystals are analyzed. The ZFS parameter values thus found are in good agreement with the EPR experiment.CF energy levels of Mn2+: NKS crystals are computed using the crystal field analysis (CFA) package. The majority of the computed and observed energy values correlate rather well. Thus, the theoretical finding verifies the experimental results.
Keywords: *Electron paramagnetic resonance, Superposition model, Zero field splitting, Crystal fields, Inorganic compounds, Single crystal.*

Date of Submission: 02-11-2026 Date of acceptance: 12-11-2026

I. Introduction

The nature of bonding and site symmetry are determined with impurity ion doping in crystals employing EPR, electron paramagnetic resonance. In crystals, doped Mn^{2+} impurity ion produces complicated EPR spectra due to its hyperfine structure splitting. Since a small deviation from higher symmetry provides appreciable change in its zero-field splitting, EPR investigations of Mn^{2+} ion doped in various crystals have been carried out extensively [1-7].

Superposition model (SPM) is an important tool for finding the local structure of the impurity ion in various crystals [8, 9]. SPM is applied for investigating the crystal field (CF) and zero field splitting (ZFS) parameters for several other applications [10–14]. SPM and the point-charge model [15, 16, 17] are often used to obtain the crystal field (CF) parameters. SPM is proposed for CF with certain assumptions as provided in [18].Using host crystal structural data, the (R_L, θ_L, Φ_L) spherical polar coordinates of each ligand are important for SPM CF analysis. When transition metal ions are added, local distortion is possibly caused by mismatches in ionic bonding, ionic size, and ionic charge. The spin-Hamiltonian parameters for Mn^{2+} and Fe^{3+} in CaO and MgO crystals have been determined [19] providing the SPM parameters which suggest the CF for 3d ions to satisfy the superposition principle. SPM intrinsic parameters based on reliable ligand distances have been evaluated for the alkali earth oxides [20].

The formula $A_2^+ B^{2+} (XO_4)_2. 6H_2O$ type crystals are in general known as Tutton salt single crystals where A is a monovalent cation, B stands for a divalent cation (usually a transition metal ion) and X represents sulfur or selenium [21–22]. Tutton salt crystals are interesting isostructural crystal family with the same monoclinic symmetry and two formula units per unit cell (Z=2) [23]. These crystals are of interest as they are widely used in UV filters [24].

Nickel potassium sulphate hexahydrate (NKS), $NiK_2 (SO_4)_2.6H_2O$ crystals belong to the Tutton salt crystal family and crystallize in the monoclinic crystal system. With high purity, suitable crystal sizes and small transparency in the UV region, they are useful in optoelectronic devices [25].

NKS is often utilized in UV light filters [26].Nickel sulphate is used in electroplating baths and for the production of other nickel compounds [27].Potassium sulphate is a high-quality potassium fertilizer and industrial chemical widely used in agriculture and specialty applications. It provides potassium and sulphur without chloride, making it ideal for chloride-sensitive crops and processes [27].The specific applications of its components are probably connected to NKS.

EPR study of Mn^{2+}doped NKS has been done at 300 K and the spin-Hamiltonian parameters are estimated [28]. The EPR spectrum displays a single set of five sextets when the magnetic field is altered in the a*c plane. This is because the a*c plane, a mirror plane normal to the b axis, is the plane where two divalent sites become equivalent. The divalent Ni^{2+} sites are occupied by the Mn^{2+} ions in the Tutton salt lattice, is therefore verified.$[Mn(H_2O)_6]^{2+}$magnetic complexes are formed when the divalent sites of the lattice of Tutton salt are replaced by Mn^{2+} ions, as indicated by angular variation studies. The orientations are discussed with the a*bc axis system, in which a* is normal to b and c.

In this work, the ZFS parameters D and E are computed for the Mn^{2+} ion in NKS at 300K (room temperature, RT)using CF parameters from SPM and perturbation equations [29]. The aim is to find the Mn^{2+} ion position in the NKS crystal as well as the distortion taking place in the lattice. The EPR experimental values match well with the Mn^{2+} ion parameters at the Ni^{2+} substitutional site in the NKS crystal with local distortion. The crystal field analysis (CFA) program and the CF parameters are used to calculate the CF energy levels in single crystals of Mn^{2+} doped NKS. The computed and observed CF energy levels correspond reasonably well. Understanding how the CF theory and SPM procedure are applicable to Mn^{2+}: NKS to get SPM parameters database is the study's further goal. Computer simulation of magnetic and spectroscopic characteristics of molecular nanomagnet (MNM) and their design will get benefit from this. The transition ion-based MNM have single-molecule magnets (SMM) [30], single-chain magnets (SCM) [31], and single ion magnets (SIM) [32].Due to MNM's interesting properties, such as magnetization's macroscopic quantum tunneling and possible applications in high-density information storage and quantum computing, the above systems have attracted many researchers [30, 31]. Different SMM or SCM systems with Mn^{2+}andCr^{3+} ions have been prepared[33].Since simpler crystal model calculations can become a foundation for complicated ones, ZFS parameter estimations for Mn^{2+}: MNMs may be performed using the model parameters discovered here. A number of crystals can be produced using this modeling technique for a range of commercial and scientific applications.

II. Crystal Structure

Crystal structure of NKS Tutton salt is monoclinic with space group $P\,2_1/a$ [34].$\beta = 105.04°$, Z = 2, b = 12.1904, c = 6.1368 and a = 9.0049 Å give the unit cell parameters. S is in the fourfold coordination (SO_4), K is in the eightfold coordination (KO_8) and Ni^{2+} is in the sixfold coordination (NiO_6) surrounded by six water oxygen ligands (OW1, OW2, OW3, OW1', OW2', OW3'). The room-temperature crystal structure of NKS and the symmetry-adapted axis system (SAAS) are shown in Fig. 1. The point group symmetry of Ni^{2+}/Mn^{2+} ions in NKS is D_{2h}.

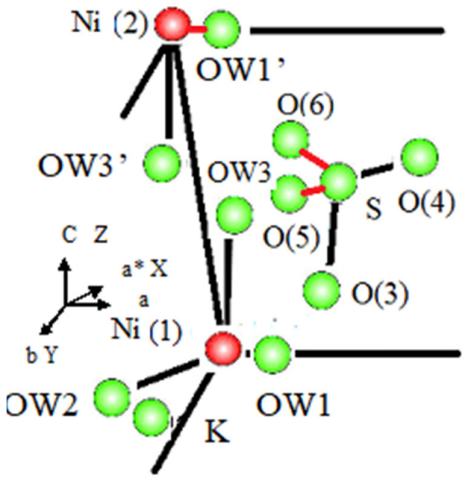

Fig. 1. The room-temperature crystal structure of NKS and the symmetry-adapted axis system (SAAS).

III. Crystal Field and Zero Field Splitting Parameter Calculations

In general, paramagnetic impurities are introduced into diamagnetic hosts to perform EPR studies. As it is normally expected that the impurity resonance lines may be broadened by the dipolar and exchange interaction of the paramagnetic host and paramagnetic impurity, the use of paramagnetic hosts is not encouraged. However, in spite of above expectation, reasonably sharp spectra have been observed in many

paramagnetic hosts [35, 36]. In the present system of Mn^{2+}: NKS also, a good EPR spectrum of impurity ion is observed [28]and so spin Hamiltonian for impurity Mn^{2+} ion only in NKS crystal is considered for analysis.

The EPR spectra of Mn^{2+}: NKS are analyzed with the spin Hamiltonian [11]:

$$E(S_x^2 - S_y^2) + D\left\{S_Z^2 - \frac{1}{3}S(S+1)\right\} + \mu_B B.g.S = \mathcal{H}(1)$$

where B, μ_B, g, D and E represent their usual meaning as given in [37–38]. For NKS, the crystallographic axis system (CAS) (a, b, c) does not form a Cartesian coordinate system. Hence, for the calculations, a modified crystallographic axis system (CAS*) (a*, b, c) must be selected [39, 40]. Modified crystallographic axes a*, b, c (a* is normal to b and c axes) and x, y, z laboratory axes are given in Fig. 1. The mutually perpendicular directions of metal-ligand bonds are taken as the local symmetry axes of the site or the symmetry adapted axes (SAA). As displayed in Fig.1, the SAAS axis-Z, which travels along the crystal c axis, is perpendicular to (X, Y). When Mn^{2+} ions are doped in NKS crystal, they replace $Ni^{2+}(1)$ sites with certain local distortion in the lattice [41].

The spin Hamiltonian for Mn^{2+} ion is taken as [41],

$$\mathcal{H}_o + \mathcal{H}_{so} + \mathcal{H}_{ss} + \mathcal{H}_c = \mathcal{H} \qquad (2)$$

$$\mathcal{H}_c = \sum B_{kq} C_q^{(k)} \quad (3)$$

where, B_{kq} and $C_q^{(k)}$ stand for the CF parameters (in Wybourne notation) and spherical tensor operators. In the orthorhombic symmetry crystal field, $B_{kq} \neq 0$ only for k = 2, 4; q = 0, 2, 4. The CF parameters, B_{kq} in NKS are obtained using SPM [42].

For SPM calculations of ZFS parameters of Mn^{2+} ions in NKS, we go to the microscopic spin Hamiltonian (MSH) expressions derived by perturbation theory [10] for the 2nd-rank ZFS parameters (D, E). The effect of the spin–orbit interaction (ζ) is taken as a perturbation to the free-ion and CF Hamiltonian, while the spin–spin interaction is neglected due to its small contribution in comparison to the spin–orbit interaction [29, 43]. The MSH approach [29, 43] gives the fourth-order perturbation contributions to the orthorhombic ZFS parameters D and E.

The site symmetry of Mn^{2+} ions in NKS crystal is orthorhombic (OR-type I) [11],for which the ZFS parameters D and E are determined as follows [43, 44]:

$$D = \left(\frac{3\zeta^2}{70P^2D'}\right)[-B_{20}^2 - 21\zeta B_{20} + 2B_{22}^2] + \left(\frac{\zeta^2}{63P^2G}\right)[-5B_{40}^2 - 4B_{42}^2 + 14B_{44}^2] \qquad (4)$$

$$E = \left(\frac{\sqrt{6}\zeta^2}{70P^2D'}\right)[2B_{20} - 21\zeta]B_{22} + \left(\frac{\zeta^2}{63P^2G}\right)[3\sqrt{10}B_{40} + 2\sqrt{7}B_{44}]B_{42} \qquad (5)$$

In above, the spin-orbit coupling parameter is provided by ζ, while the Racah parameters are shown by C and B and G = 10B+5C, P = 7B+7C, D' = 17B+5C. TakingN, the average covalency parameter, $\zeta = N^2\zeta_0$, $B = N^4B_0$, $C = N^4 C_0$, where ζ_0 is free ion spin-orbit coupling parameter and B_0 and C_0arefree ion Racah parameters[42, 45]. $\zeta_0 = 336$ cm^{-1},$B_0 = 960$ cm^{-1} and $C_0 = 3325$ cm^{-1}for free Mn^{2+} ion[11].

In terms of Racah parameters, N is obtained from ($\sqrt{B/B_0} + \sqrt{C/C_0}$)/2 = N. The Racah parameters (B = 850 cm^{-1}, C = 2970 cm^{-1}) are found from optical study of Mn^{2+} ion in zinc cesium sulphate hexahydrate where ligands are oxygens [46], since no optical absorption study of Mn^{2+}dopedNKSisgiven in literature. [Mn $(H_2O)_6]^{2+}$ complexes are formed when the Mn^{2+} ion replaces the divalent sites of Zn^{2+} in zinc cesium sulphate hexahydrate and the optical absorption spectra are because of [Mn $(H_2O)_6]^{2+}$complexes [41]. As the same complex forms in Mn^{2+}doped NKS, its optical absorption spectra will conform to those of Mn^{2+}: zinc cesium sulphate hexahydrate. For SPM analysis ofMn^{2+} in $BiVO_4$ [43] Yoem et al. have used optical spectra of Mn^{2+}: MgO due to similar ligands in the crystal. Therefore, for Mn^{2+}doped NKS crystal, it seems appropriate to use the Mn^{2+} optical absorption data in zinc cesium sulphate hexahydrate.

The CF parameters are estimated using SPM [18, 43], with co-ordination factor $K_{kq}(\theta_j, \varphi_j)$ and intrinsic parameter $\overline{A_k}(R_j)$, given by

$$\sum_j K_{kq}(\theta_j, \phi_j)\, \bar{A}_k(R_j) = B_{kq} \qquad (6)$$

$\overline{A_k}(R_j)$ is obtained from the relation

$$\overline{A_k}(R_0)\left(\frac{R_0}{R_j}\right)^{t_k} = \bar{A}_k(R_j) \qquad (7)$$

where the parameters $\overline{A_k}(R_0)$, R_0,t_k and R_j are discussed in [43]. For Mn^{2+}doped crystals, $t_2 = 3$ and $t_4 = 7$have been used by earlier workers[43], the same values are taken here for Mn^{2+}: NKS crystal. Since the co-ordination about Mn^{2+}ion is octahedral, $\overline{A_4}$ is evaluated from the relation [43]

$$\overline{A_4}(R_0) = \frac{3}{4} Dq \qquad (8)$$

The optical study [46] yields Dq = 790 cm^{-1}, which gives $\overline{A_4}(R_0)$ = 592.5 cm^{-1}. For $3d^5$ ions the ratio $\frac{\overline{A_2}}{A_4}$ lies in the range 8 - 12 [42, 43-49]. With $\overline{A_2}$ =10 $\overline{A_4}$, 5925 cm^{-1} = $\overline{A_2}$ .is obtained.

IV. Results and Discussion

From the arrangement of ligands about Mn^{2+} ion (Fig. 1) and SPM, the Mn^{2+} ion's CF characteristics at the Ni^{2+} sites in NKS are computed. For site I in the single crystal of NKS, Table 1 shows the coordinates of atoms, bond length R (with and without distortion) and angles θ, φ. The CF and ZFS parameters as well as R_0 are shown in Table 2. Table 2 gives that R_0 = 0.200 nm being slightly less than the sum of radii of ions(0.223 nm) of Mn^{2+} = 0.083 nm and O^{2-} = 0.140 nm with no distortion and $\frac{\overline{A_2}}{A_4}$ = 8, 10, 12 yield ZFS parameter values at octahedral substitutional site I to be largely different from the EPR experimental ones[28]. Experimental ZFS parameters |D| and |E| (10^{-4} cm^{-1}) obtained from EPR measurement are 422.5, 38.7, respectively. |E|/|D| is found as 0.091which is smaller than the standard value 0.33 [38]. With no distortion considered, |D| and |E| obtained are greater than the EPR measurement values. |E|/|D| is also larger than the standard value 0.33 [38]. Local distortion is, therefore, introduced in the calculation. For local distortion an iterative process as in [44] has been used by changing R, θ and φ to minimize the difference between calculated and experimental D and E and E/D reaching to standard value 0.33[38] with lattice strain being minimum. Using local distortion and above R_0, the substitutional octahedral sites' ZFS parameters are computed for $\frac{\overline{A_2}}{A_4}$ =8, 10, 12 and are listed in Table 2. The ZFS parameter |D| is smaller than the experimental value (error 22.8 %),|E| is greater than the experimental one (error 149.6%) for $\frac{\overline{A_2}}{A_4}$ =8 while both |D| and |E| are greater for $\frac{\overline{A_2}}{A_4}$ =12 (error 26.6% for D and 397.4 % for E). |E|/|D| is smaller than 0.33 (the standard value)for $\frac{\overline{A_2}}{A_4}$ =8 and greater for $\frac{\overline{A_2}}{A_4}$ =12, while |D| is in good agreement with the EPR experimental value and |E| is greater than the experimental value for $\frac{\overline{A_2}}{A_4}$ =10 [28] but |E|/|D| comes out to be equal to the standard value 0.33 [38].Hence $\frac{\overline{A_2}}{A_4}$ =10 seems to be quite appropriate. The

power law exponent parameters $t_2 = 3$ and $t_4 = 7$ with transformation S2 for standardization [38] have been used to obtain |E|/|D| ratio equal to 0.33 and calculated ZFS parameters very near to experimental values estimated from EPR. Similar value of $\frac{\overline{A_2}}{A_4}$ has been used for Mn^{2+}doped diglycine calcium chloride tetrahydrate [50], Fe^{3+} doped $BiVO_4$ [42] and Mn^{2+} doped ZKS single crystals[44].

Table 1. Coordinates of atoms, bond length R and θ, φ angles in NKS (site I).

Position of Mn^{2+}Ligands	Spherical polar coordinates of ligands								
		x (Å)	y	z	R(nm)	θ°		φ°	
		Without distortion							
Site : Substitutional	OW1	0.16694	0.11095	0.1630	0.20759	R_1	85.49	θ_1 85.37	φ_1
Zn(1)	OW2	- 0.16659	0.11244	0.0356	0.20849	R_2	89.02	θ_2 94.58	φ_2
(0.0000, 0.0000,	OW3	0.00028	- 0.06662	0.3016	0.20206	R_3	81.41	θ_3 89.99	φ_3
0.0000)	OW1'	-0.16694	-0.11095	-0.1630	0.20759	R_4	94.50	θ_4 94.62	φ_4
	OW2'	-0 .16694	0.38905	0.6630	0.66693	R_5	84.29	θ_5 91.44	φ_5
	OW3'	0.16694	0.61095	0.3370	0.77712	R_6	87.51	θ_6 88.76	φ_6
		With distortion							
I	OW1				0.24759		65.49	81.37	
	OW2				0.25371		69.02	98.58	
	OW3				0.26206		61.41	91.99	
	OW1'				0.27759		74.50	96.12	
	OW2'				0.75193		74.29	93.44	
	OW3'				0.86212		83.51	86.76	

Table 2. Mn^{2+}doped NKS crystal: ZFS and CF parameters.

		Parameters of CF (cm^{-1})					Parameters of ZFS ($10^{-4}cm^{-1}$)		
Site	R_0(nm)	B_{20}	B_{22}	B_{40}	B_{42}	B_{44}	|D|	|E|	|E|/|D|
		Without distortion							
Site I $\frac{\overline{A_2}}{A_4}$ = 8	0.200	-16995.0	-20998.8	5192.393	5528.984	8017.853	3270.6	1665.8	0.509
$\frac{\overline{A_2}}{A_4}$ =10	0.200	-21243.8	-26248.5	5192.393	5528.984	8017.853	4689.9	2402.2	0.512
$\frac{\overline{A_2}}{A_4}$ =12	0.200	-25492.5	-31498.2	5192.393	5528.984	8017.853	6411.5	3289.2	0.513
		With distortion							
Site I $\frac{\overline{A_2}}{A_4}$ = 8	0.200	-6868.11	2772.827	-298.715	-81.8618	2763.488	326.1	96.6	0.296
$\frac{\overline{A_2}}{A_4}$ =10	0.200	-8585.14	3466.034	-298.715	-81.8618	2763.488	422.5	140.5	0.333
						Exp.	422.5	38.7	0.091
$\frac{\overline{A_2}}{A_4}$ =12	0.200	-10302.2	4159.241	-298.715	-81.8618	2763.488	535.0	192.5	0.359

The CFA package [51] and CF parameters B_{kq} (with distortion) are used to calculate the optical spectra of Mn^{2+}doped NKS single crystals. The total Hamiltonian is diagonalized in order to find the CF energy levels of the Mn^{2+} ion,

Table 3 lists the CF energy levels (observed and calculated) for substitutional site [46]. From the characteristic and the position of the bands observed, they have been attributed to a Mn^{2+} ion in octahedral symmetry [44, 46, 52]. The assignment of different bands has been done as in [44, 53]. CFA package [51] can perform diagonalization of the total Hamiltonian within the $3d^N$ basis of states in the intermediate crystal field coupling scheme yielding the CF energy levels and the state vectors. The spin–spin interaction (M_0), Trees correction (α), the spin–orbit interaction (ζ), and the spin-other orbit interaction (M_{00}, $M_{22;}$ two parameters),the Coulomb interaction (using Racah B and C parameters), the Hamiltonian of the crystal field are all considered for the Hamiltonian of CFA package. The following free-ion parameter values are taken in the CFA computations: B = 850 and C = 2970, ζ_0 = 336, α = 76 cm^{-1}, M_{00} = 0.2917, M_{22} = 0.0229, M_0 = 0.2917 and M_2 = 0.0229. The complete Mn^{2+}spectra consist of 120 degenerate states, only a few energy levels based on intensity are shown here [44, 53]. The transitions pertaining to$^4T_{2g}$(G), $^4T_{1g}$(G)and $^4T_{1g}$(P) exhibit greater deviation than those pertaining to $^4A_{1g}$(G), ^4E_g(G), $^4T_{2g}$(D), ^4E_g(D), $^4A_{2g}$(F), and $^4T_{1g}$(F). The causes for larger deviations of above transitions may be vibronic coupling, electron correlation effects or limitations of the CF model [41].The optical absorption spectra of Cr^{3+}-activated phosphors have been understood using Franck-Condon analysis with the configurational-coordinate (CC) model [54]. The different excited state-ground state transitions in Cr^{3+} are a result of the lattice vibrations' strong coupling (CC model) [54]. The CC model has not been used here and so there is difference between excited-state peak energies obtained and energies of the zero-phonon line (ZPL) [54, 55].

Table 3. Energy levels (calculated and observed) in single crystal of Mn^{2+}: NKS.

Transition from state $^6A_{1g}$(S)	Observed (cm^{-1})	Calculated (cm^{-1})
		I
$^4T_{1g}$(G)	18436	23141, 23195, 23344, 23441, 23459, 23508
$^4T_{2g}$(G)	22815	23737, 23768, 24147, 24182, 24249, 24282
^4E_g(G)	24783	24832, 24850, 24858, 24876
$^4A_{1g}$(G)	24850	24877, 24881
$^4T_{2g}$(D)	28003	26895, 26949, 28326, 28341, 29344, 29434
^4E_g(D)	29870	29717, 29860, 30198 30283
$^4T_{1g}$(P)	32435	31928, 31942, 34786, 34978, 35037, 35192
$^4A_{2g}$(F)		36524, 36831
$^4T_{1g}$(F)	41460	41176, 41271, 41330, 41632, 41684, 42653

Table 3 demonstrates that the calculated and observed energy levels are in reasonable conformity. So, the theoretical study validates the EPR experimental result [28, 46] that Mn^{2+} ions enter the NKS crystal at substitutional Ni^{2+}octahedral site. The obtained model parameters of this research can be applied to ZFS parameter evaluations of Mn^{2+} ions in molecular nanomagnets at similar sites. The modeling process employed here may be useful in exploring crystals having numerous applications in science and industry.

V. Conclusions

The splitting parameters for zero field and crystal field for Mn^{2+} ion doped NKS single crystals are found utilizing perturbation expressions and superposition model. The zero field splitting parameters calculated for $\frac{\overline{A_2}}{A_4}$ =10 validate the results of the EPR experiment. The computed CF energy levels and the values from the experiment are reasonably in agreement. Consequently, the result of EPR experiment that Mn^{2+} ions replace Ni^{2+} sites in NKS crystal is theoretically confirmed. The parameters of ZFS for Mn^{2+} ions in molecular nanomagnets at similar locations can be obtained using the model parameters of the current study. The present modeling method may be helpful in exploring several crystals having numerous applications in science and industry.

Acknowledgement

The author is grateful to Prof. C. Rudowicz of Faculty of Chemistry, Adam Mickiewicz University in Poznan, Poland, for the CFA program, and the Head of the Physics Department, University of Allahabad in Prayagraj for making available departmental amenities.

Declarations

Ethical Approval:

No animal or human subjects were used in this investigation, and it has not been performed in any private or protected places. Corresponding places did not need specific approvals.

Competing interests:

The author certifies that none of the work presented in this paper could have been influenced by competing personal relationships or financial interests.

Authors' contributions:

Ram Kripal: concept and oversight, wrote the manuscript, prepared the figure and carried out the computations.
.

Funding:

There has been no funding.

Availability of data:

The data are available on request from the author.

References

[1] R. Murugesan, V. S. X. Anthonisamy, and S. Subramanian, Single Crystal EPR Study of Mn (II) doped cis-Catena- sulphatoaquo-tris(imidazole) cadmium(II), Mn (II) in imidazole ligated low symmetry site, Spectrochim. Acta A 49 (1993) 1801-1807.
[2] J. A. Weil, J. R. Bolton, Electron Paramagnetic Resonance: Elementary Theory and Practical Applications; 2nd ed., Wiley, New York, 2007.
[3] P. S. Rao, Single crystal EPR study of Mn(II)-doped magnesium potassium Tutton's salt, Spectrochim. Acta A 49(1993)897-901.
[4] S. K. Misra, Estimation of the Mn^{2+} zero-field splitting parameter from a polycrystalline EPR spectrum, Physica B 203 (1994) 193-200.
[5] S. N. Rao, Y. P. Reddy, and P. S. Rao, Spectroscopic studies of manganese doped cadmium maleate dihydrate, Solid State Commun. 82 (1992) 419-426.
[6] D. Halder, Y. Jana, D. Piwowarska, P. Gnutek, C. Rudowicz, Tailoring single-ion magnet properties of coordination polymer C11H18DyN3O9 (Dy-CP) using the radial effective charge model (RECM) and superposition model (SPM), Phys. Chem. Chem. Phys.26(2024) 19947-19959.
[7] S. P. Rathee, S. S. Hooda, EPR and superposition-model analysis of zero-field splitting parameters for Mn^{2+} doped in $ZnNbOF_5.6H_2O$ and $CoNbOF_5.6H_2O$ single crystals, Indian J. Phys. 99(1)(2025)145-148.
[8] V. K. Jain, G. Lehmann, Electron Paramagnetic Resonance of Mn^{2+} in Orthorhombic and Higher Symmetry Crystals, Phys. Status Solidi b 159(1990) 495-544.
[9] D. J. Newman, Superposition model analysis of spin Hamiltonian parameters, J. Phys. C: Solid State Phys. 15(1982) 6627-6630.
[10] C. Rudowicz, P. Gnutek, M. Açıkg¨oz, Superposition model in electron magnetic resonance spectroscopy – a primer for experimentalists with illustrative applications and literature database, Appl. Spectrosc. Rev. 54 (2019) 673–718.
[11] A. Abragam, B. Bleaney, Electron Paramagnetic Resonance of Transition Ion, Dover, New York, 1986.
[12] J.R. Pilbrow, Transition-Ion Electron Paramagnetic Resonance, Clarendon Press, Oxford, 1990.
[13] B.G. Wybourne, Spectroscopic Properties of Rare Earth, Wiley, New York, 1965.
[14] J. Mulak, Z. Gajek, The Effective Crystal Field Potential, Elsevier, Amsterdam, 2000.

[15] R. Bo˘ca, Zero-field splitting in metal complexes, Coord. Chem. Rev. 248 (2004) 757–815.
[16]. M. G. Brik, N. M. Avram (Eds.). Optical Properties of 3d-Ions in Crystals: Spectroscopy and Crystal Field Analysis. Heidelberg: Springer, (2013), Y. Y. Yeung: Chapter 3, pp. 95-121.
[17] A. K. Yadav, U. M. Tripathi, and R. Kripal, Theoretical Calculation of Zero-Field Splitting Parameters for Mn^{2+} in Potassium Hydrogen Sulphate, Appl. Magn. Reson.53 (2022) 941–947.
[18] D. J. Newman and B. Ng, The superposition model of crystal fields, Rep. Prog. Phys. 52 (1989) 699-763.
[19] D. J. Newman, E. Siegel**,** Superposition model analysis of Fe^{3+} and Mn^{2+} spin-Hamiltonian parameters, J. Phys. C: Solid State Phys. 9 (1976)4285-4292.
[20] Y. Y. Yeung, Local distortion and zero-field splittings of $3d^5$ ions in oxide crystals, J. Phys. C: Solid State Phys. 21 (1988)2453-2462.
[21] H. T. Montgomery, E.C. Lingafelter, The crystal structure of Tutton's salts. I. Zinc ammonium sulfate hexahydrate, Acta Cryst. 17(1964) 1295–1299.
[22] M. Wildner, D. Marinova, D. Stoilova, Vibrational spectra of $Cs_2Cu(SO_4)_2{\cdot}6H_2O$and $Cs_2Cu(SeO_4)_2{\cdot}nH_2O$(n=4, 6) with a crystal structure determination of the Tutton salt $Cs_2Cu(SeO_4)_2{\cdot}6H_2O$,J. Mol. Struct. 1106(2016) 440–51
[23] H. T. Montgomery, E. C. Lingafelter, The crystal structure of Tutton's salts. II. Magnesium ammonium sulfate hexahydrate and nickel ammonium sulfate hexahydrate Acta Cryst. 17(1964) 1478–9
[24] M.de Oliveira, S. Ghosh, T. S. Pacheco, G. J. Perpétuo, C. J. Franco, Growth and structural analysis of ammonium nickel cobalt sulfate hexahydrate crystals, Materials Research Express 4(2017) 105036
[25] A. Abu El-Fadl, A. M. Nashaat, Growth, structural, and spectral characterizations of potassium and ammonium zinc sulfate hydrate single crystals, Appl. Phys. A123 (2017) 339(11 pages).
[26]D. L. Perry, Handbook of Inorganic Compounds, CRC Press, Boca Raton, Florida, USA, 2016.
[27] Y. Hea, J. Chenb, G. Sua, X. Zhuanga, G. Leea, R. Jiang, Growth of potassium nickel sulfate hexahydrate (KNSH) crystal and its characterization, J. Cryst. Growth 233 (2001) 809–812.
[28] R. S. Saraswat, G. C. Upreti, Spin Quenching and EPR of Mn^{2+} in Single Crystals of Nickel Salts, Physica B, 92(1977)253-257.
[29] W. L. Yu, M.G. Zhao, Spin-Hamiltonian parameters of ^6S state ions,Phys. Rev. B 37(1988)9254-9267.
[30] G. Aromí, E. K. Brechin, Synthesis of 3d metallic single-molecule magnets, Struct. Bonding 122 (2006) 1-67.
[31] C. Coulon, H. Misayaka, R. Clérac, Single-Chain Magnets: Theoretical Approach and Experimental Systems, Struct. Bonding 122 (2006) 163-206.
[32] M. Murrie, Cobalt (II) single-molecule magnets, Chem. Soc. Rev. 39 (2010) 1986-1995.
[33] C. van Wüllen, Magnetic anisotropy through cooperativity in multinuclear transition metal complexes: theoretical investigation of an anisotropic exchange mechanism, Mol. Phys. 111 (2013) 2392–2397.
[34] F. Bosi, G. Belardi, P. Ballirano, Structural features in Tutton's salts $K_2[M^{2+}(H_2O)_6](SO_4)_2$, with M^{2+} = Mg, Fe, Co, Ni, Cu, and Zn, Am. Mineral., 94(2009) 74–82.
[35] N. O. Gopal, K. V. Narsimhulu, J. L. Rao, EPR and IR spectral studies on Mn^{2+} ions in nickel maleate tetrahydrate single crystals, J. Phys. Chem. Solids 63(2002)295-302
[36] S. K. Misra, J. Sun, X. Li, EPR and optical absorption studies of a VO^{2+} -doped $Co(NH_4)_2(SO_4)_2{\cdot}6H_2O$ single crystal: Spin-lattice relaxation time of the host Co^{2+} ions and systematics of EPR spectra in VO^{2+} -doped $M(NH_4)_2(SO_4)_2{\cdot}6H_2O$ (M = Co, Zn, Cd, Mg, Fe) single crystals, Physica B, 168(1991)170-176.
[37] C. J. Radnell, J. R. Pilbrow, S. Subramanian, M. T. Rogers, Electron paramagnetic resonance of Fe^{3+} ions in $(NH_4)_2SbF_5$. J. Chem. Phys. 62(1975)4948-4952.
[38] C. Rudowicz, R. Bramley, On standardization of the spin Hamiltonian and the ligand field Hamiltonian for orthorhombic symmetry. J. Chem. Phys. 83(1985) 5192- 5197.
[39] N. Das , R. Ghosh, Y. M. Jana, J. Saha, S. Khatun , S. Nandi, A. Tripathi , H. C. Gupta, Y. Y. Yeung, M. Açıkgöz , C. Rudowicz, Infrared, Raman, and site-selective spectra of Nd^{3+} ions doped in melilites $A_2TGe_2O_7$, expounded by computational modelling of crystal-field parameters, energy levels, and lattice dynamics, Physica B, 724(2026) 418153.
[40] Y. M. Jana, A. Biswas, D. Halder, S. Sarkar, C. Rudowicz, Exploring crystal field influences on optical spectra of $3d^7$ (Ni^{3+} vs Co^{2+}) ions in cubic pyrochlores $A_2Ti_2O_7$ (A = Y, Gd) and layered-hexagonal MCl_2 (M = Cd, Mg) for potential optoelectronic applications, J. Solid State Chem., 345 (2025) 125241.
[41] B. N. Figgis, M. A. Hitchman, Ligand Field Theory and its Applications; Wiley, New York, 2000.
[42] T. H. Yeom, S. H. Choh, M. L. Du, M. S. Jang, EPR study of Fe^{3+} impurities in crystalline $BiVO_4$.Phys. Rev. B 53(1996) 3415-3421.
[43] T. H. Yeom, S. H. Choh, M. L. Du,A theoretical investigation of the zero-field splitting parameters for an Mn^{2+} centre in a $BiVO_4$ single crystal.J. Phys.: Condens. Matter 5(1993)2017-2024.
[44] M. Bharati, V. Singh, R. Kripal, Local structure, zero field splitting and optical absorption of Mn^{2+} doped $ZnK_2(SO_4)_2{\cdot}6H_2O$ single crystals, Mat. Adv.6(2025)8930-8935.
[45] C. K. Jorgensen, Modern Aspects of Ligand Field Theory; North- Holland, Amsterdam, 1971, p.305.
[46]K. Purandar, J. L. Rao, S. V. J. Lakshman, Optical Absorption Spectrum of Mn^{2+} in Zinc Cesium Sulphte Hexahydrate, Acta Phys. Slov. 34(1984)195-207.
[47] D. J. Newman, B. Ng (Eds.), Crystal Field Handbook; Cambridge University Press, Cambridge, 2000.
[48]A. Edgar, Electron paramagnetic resonance studies of divalent cobalt ions in some chloride salts. J. Phys. C: Solid State Phys. 9(1976)4303-4314.
[49] R. Kripal, M. G. Misra, A. K. Yadav, P. Gnutek, M. Açıkgöz, C. Rudowicz, Theoretical Analysis of Crystal field Parameters and Zero field Splitting Parameters for Mn^{2+} ions in Tetramethylammonium Tetrachlorozincate, Polyhedron, 235(2023)116341.
[50] S. Pandey, R. Kripal, A Theoretical Analysis of Zero Field Splitting Parameters of Mn^{2+}Doped Diglycine Calcium Chloride Tetrahydrate, Chin. J. Phys. 52(2014) 262-271.
[51]Y. Y. Yeung, C. Rudowicz, Crystal Field Energy Levels and State Vectors for the $3d^N$ Ions at Orthorhombic or Higher Symmetry Sites. J. Comput. Phys. 109(1993)150-152.
[52] Y. Tanabe, S. Sugano, On the Absorption Spectra of Complex Ions. I, J. Phys. Soc. Jpn.9 (1954)753-766.
[53] Y.Y. Yeung, C. Rudowicz, Y.M. Chang, J Qin, Model calculation of the spectroscopic properties for Cr^{3+} Kyanite, J. Lumin. 60&61 (1994) 108-111.
[54]S. Adachi, Photoluminescence Spectroscopy and Crystal-Field Parameters of Cr^{3+} Ion in Red and Deep Red-Emitting Phosphors, ECS J. Solid State Sci. Tech., 8(2019)R164.
[55] S. Adachi,Review—Photoluminescence Properties of Cr^{3+}-Activated Oxide Phosphors, ECS J. Solid State Sci. Tech., 10(2021) 026001.